

# Final Fall Report

## Team 13

### Designing & Testing a Lightweight Heatsink for PV Converter



#### Members:

Melanie Gonzalez	mtg12c
Leslie Dunn	lvd12b
James Hutchinson	jrh12c
Tianna Lentino	tnl13
Colleen Kidder	cmk13

#### Faculty Advisor/s

Dr. Hui Li

Dr. Juan Ordonez

#### Sponsor/s

The Center for Advanced Power Systems (CAPS)

Aero-Propulsion, Mechatronics and Energy (AME)

PowerAmerica – U.S. Department of Energy

#### Instructor/s

Dr. Chiang Shih

Dr. Jerris Hooker

**December 5, 2016**

## Table of Contents

<b>Table of Figures</b> .....	<b>iii</b>
<b>Table of Tables</b> .....	<b>iii</b>
<b>ABSTRACT</b> .....	<b>iv</b>
<b>ACKNOWLEDGMENTS</b> .....	<b>v</b>
<b>1. Introduction</b> .....	<b>1</b>
<b>2. Project Definition</b> .....	<b>2</b>
2.1 Problem Statement .....	2
2.2 Background Research.....	2
2.3 Customer’s Need Statement .....	6
2.4 Project Objectives and Goals .....	6
2.5 Project Constraints .....	7
<b>3. Scheduling</b> .....	<b>7</b>
<b>4. Resource Allocation</b> .....	<b>10</b>
<b>5. Product Specification</b> .....	<b>11</b>
5.1 Design Specification .....	11
5.2 Performance Specification .....	11
<b>6. Conceptual Design</b> .....	<b>12</b>
6.1 Emulated Heat Source .....	12
6.1.1 Testing of Emulated Heat Source .....	12
6.2 Heatsink Design .....	13
6.3 Heatsink Optimization .....	19
<b>7. Procurement</b> .....	<b>21</b>
<b>8. Risk Assessment</b> .....	<b>22</b>
<b>9. Conclusion</b> .....	<b>23</b>
<b>References</b> .....	<b>24</b>
<b>Biography</b> .....	<b>25</b>
<b>Appendix A: Plate Fin Calculations</b> .....	<b>26</b>
<b>Appendix B: Pin Fin Calculations</b> .....	<b>31</b>

## Table of Figures

Figure 1 – Responsibilities of EE and ME Students.....	7
Figure 2 – Gantt Chart.....	9
Figure 3 – Heat Sink designed by CAPS researchers.....	11
Figure 4 – Bi-modular Pin Fin Design.....	15
Figure 5 – Important geometric features of staggered pin fin heatsink.....	16
Figure 6 – Brace for Pin Fin Design.....	16
Figure 7 – Bi-modular Plate Fin Design.....	17
Figure 8 – Important geometric features of plate fin heatsink.....	18
Figure 9 – Parameters that affect Thermal Resistance & Weight.....	20

## Table of Tables

Table 1 – Work Breakdown Structure.....	8
Table 2 – Plate Fin & Pin Fin Geometric Parameters.....	14
Table 3 – Budget Information for Team 13.....	22

## ABSTRACT

It is necessary to keep power electronic devices from overheating to prevent failure. In order to do so, heatsinks are used to dissipate the heat that is generated from the chip. This report delves into the testing and development of a lightweight aluminum heatsink that will be used for dissipating heat from the power modules of a new photovoltaic inverter that is being developed at the Florida State University Center for Advanced Power Systems. Team 13 focuses on studying forced convective aluminum heatsinks with two fin designs: cylindrical pin fins and rectangular plate fins. In this report, testing protocol is developed with a heat source emulator. In order to improve the power density of the PV inverter, the heatsink weight and thermal resistance must be reduced. Calculations for determining the thermal resistance of pin fin and plate fin configurations are included and the procedure for determining the optimum design is described.

## ACKNOWLEDGMENTS

Team 13 would like to express gratitude to Dr. Li for the opportunity to work on the Designing and Testing of Heatsinks as well as for providing assistance through her graduate students and laboratory space to conduct project proceedings. Team 13 would also like to thank the graduate students, specifically to Thierry Kayiranga, for providing feedback and support on this project.

Thank you to Dr. Wei Guo and Dr. Juan Ordonez for providing insight and assistance with challenges faced by the team.

Thank you to the FAMU-FSU College of Engineering, Mechanical Engineering Department, and Electrical Engineering Department for providing the knowledge needed to participate in the Senior Design. Thanks to FSU CAPS and AME, as well as Power America for sponsoring the project.

Lastly, Team 13 gives thanks to Dr. Shih and Dr. Hooker for coordinating the team configuration and providing the guidelines needed for a successful semester ahead.

# 1. Introduction

This senior design project focuses on creating a cost effective, lightweight heatsink in order to improve the power density of a PV inverter and make future power electronic converters more efficient. This project is sponsored by The Center of Advanced Power Systems (CAPS) under Dr. Hui “Helen” Li. This project is directly related to the research of a current Ph.D. candidate, multiple graduate students working under Dr. Li have been available for questions regarding the nature of it. Along with providing expertise and advice, the graduate students have assisted with gathering materials needed for the testing and prototyping.

The PV inverter at CAPS has a power density of 2.5 kW/kg, and this senior design team hopes to help improve this power density by reducing the weight of the heatsink for the system. The current heatsink that CAPS is using for testing the PV inverter is oversized. It has 8 power modules on it which must be kept below a certain temperature, and it weighs 6.5 kg. The team of graduate students that are involved with designing it knew that the heatsink they’re using is oversized because the bottom of the heatsink is “cold to the touch” during operation.

Team 13’s design of a lighter heatsink will be completed by mid-December, 2016. The reason for the time-critical nature of this prototype is because the team will be attending the Power America conference occurring January 17<sup>th</sup>, 2017 at North Carolina State University. The team plans to show simulation results for a cylindrical pin fin heatsink, but still continues to compare simulation and testing results for both plate a fin and pin fin configurations.

The overall design and manufacturing plan for the lightweight PV converter and thermal testing was broken up into four stages in order to achieve the best results possible. Stage one included all background research into power switches, power converters, switching loss calculations, heatsink configurations, materials, air flow, etc. Stage two included separate but simultaneous efforts between the electrical engineering students and the mechanical engineering students to begin the simulation process of the project. The mechanical engineering students developed a procedure for calculating the thermal resistance of different heatsink configurations. The electrical engineering students will perform power loss calculations in order to provide these

results to the mechanical engineering students who are designing and configuring the smaller, lightweight heatsink. Stage three includes testing different heatsink configurations to confirm the simulation results, and stage 4 involves optimizing and implementing the final design. Team 13 has completed stage 1, and has made significant progress on stages 2 and 3. Stage 4 will begin after the conference.

## 2. Project Definition

The following subsections address the needs of the customer for the design and any constraints or concerns that needed to be considered when planning and designing. These constraints include any physical parameters that must be achieved in order to meet requirements set by the customer. Research on power loss calculations and on the design and optimization of heatsinks is summarized to better understand the challenges that have been overcome in the power engineering field and to further develop ideas for this project.

### 2.1 Problem Statement

In current research and development of power converters, the total weight of the system is a concern due to large, heavy heatsinks. Team 13 is required to redesign the heatsink component of a PV converter so that the system weight is reduced and the power density is increased. To test the heatsink, an emulated heat source has been created.

### 2.2 Background Research

#### 2.2.1 Introduction to Power Loss Calculations

Switching losses in power MOSFETs are the dominant power loss in power electronic converters. Parasitic capacitances in power MOSFET include gate-source capacitance, gate-drain capacitance, and drain source capacitance. To calculate the switching loss for a power MOSFET, a common expression used is  $P_{sw} = \frac{1}{2} V_D I_D (t_{off} + t_{on}) f + \frac{1}{2} C_{oss} V_D^2 f$  [1].  $C_{oss}$  is the output capacitance given by  $C_{oss} = C_{GD} + C_{DS}$  [1] and is thought to introduce the heating of the MOSFET

during turn-on through dissipation of energy. This energy was initially stored in the capacitor during the turn-off cycle. While these equations for calculating switching losses are widely accepted and used, they are not as accurate as other methods [1].  $C_{oss}$ , the term for calculating the switching power loss, overestimates the turn-off switching loss and underestimates the turn-on switching loss [1]. The overestimation and underestimation do not cancel each other out, and in turn they introduce erroneous error. However, since the net power loss contribution from  $C_{oss}$  is minimal, this term can be ignored in power loss calculations.

Another error introduced in common power loss calculations is when  $V_{DS}$  is approximated as a linear waveform, which is introduced by the switching power loss from the equation above. Instead, defining the gate charge  $Q_{sw}$  as  $Q_{sw}^*$  allows us to neglect the gate charge increment accounting for the gate voltage that was still in the plateau. Using the gate current  $I_{GS}^* = V_{gs} - V_P/R_g$  and  $Q_{sw}^*$ , the switching power loss can be further estimated in a more accurate model. It is important to note that in this paper, the parasitic inductance loss in power MOSFETs is not explored and this also constitutes a significant loss.

A newer switching device that is being investigated is the Silicon Carbide (SiC) MOSFET. The SiC MOSFET introduces smaller parasitic capacitance while higher switching speed are achieved. Higher switching speeds contribute to the lowering of losses in switching devices by reducing the losses in the switching cycle, which is where most losses occur. A method for calculating power loss is to assume that the gate driver is an ideal voltage source and that the common source stray inductance,  $L_s$ , and gate resistance are varied. A model is used to simulate the switching capability of the SiC MOSFET. Due to the fact that the parasitic capacitance is listed in the datasheets as combinations of the MOSFET port capacitances and the fact that these port capacitances play different roles in the switching cycle, these capacitances must be taken into account separately for the model to be as accurate as possible. During the turn-on switching, two things happen: the current rises rapidly through the MOSFET and the voltage drops. The two currents that are observed are the drain current and the channel current. The channel current contributes significantly more than the drain current, specifically in the falling voltage region. This



channel current surge is due to the discharging of  $C_{ds}$  and  $C_{gd}$ , which were charged during turn-off, so that during turn-on voltage fall phase. Channel current = load current + discharge current of  $C_{ds}$  + discharge current of  $C_{gd}$  [2]. This charging and discharging can be viewed in terms of energy as  $E_{on} = E_{on}(\text{measured}) + E_{oss}$ , where  $E_{oss}$  is the energy stored in  $C_{oss} = C_{gd} + C_{ds}$ . The measured energy is calculated by integrating voltage and current that is measured. These various methods and techniques for calculating power loss offer better insight into possible solution methods for Team 13.

Although these analytical methods provide many calculations to determine the switching loss, another method which can be easier is to use the switching waveform. The switching waveform can show the nonlinear behavior of the switching devices. Through the use of nonlinear approximation methods, the switching waveform can easily determine the total switching loss.

## 2.2.2 Introduction to Heatsink Design

The purpose of a heat sink is to transfer heat generated by a source to the environment, so that a device is properly maintained and does not overheat. Creating heat sinks that are smaller in size and weight but that still effectively transfer heat is critical as technology advances. Important factors in the heat sink design that will affect its performance include the overall dimensions of the heat sink, the properties of the material used, and the size, shape, and number of fins used. Conduction, heat transfer through a material, and convection, heat transfer through a moving fluid, are both involved in the thermal analysis of a heat sink. Heat sinks can operate by natural convection or, if fans are used, by forced convection. In order to optimize heat sink performance, various fin types have been developed. A study by Annuar and Ismail compared many different configurations of pin fins including inline, staggered, and randomized [3]. Pin fins were shown to dissipate heat better than plate fins. The inline arrangement resulted in smooth airflow; the staggered arrangement had a little better heat transfer performance but resulted in turbulent airflow. The randomized arrangement combined the effects of inline and staggered and resulted in the best thermal performance. A study by Drogenik, Stupar, and Kolar compared heat sinks made

out of different materials in order to optimize heat sink performance [4]. The advanced composite materials with high thermal conductivities were not found to have significantly better cooling results than aluminum and copper. Aluminum was found to be the most reasonable option due to its weight, cost, and manufacturability. The thermal performance of a heat sink design can be analyzed using the finite element method (FEM) through software such as COMSOL Multiphysics.

In a study by Ning, Lei, Wang, and Ngo, an analytical model was developed to optimize a heatsink-fan system to reduce the total weight of the cooling apparatus [5]. The heat sink design chosen for analysis was the plate fin heatsink made of aluminum with a cooling fan blowing horizontally along the fins. The design parameters that contribute to the total weight of the system were found to be the heatsink length, fin number, fin height, fin width, channel width and the weight of the fan being used. The MATLAB optimization toolbox was used to optimize the heatsink-fan system based on the parameters previously given. The dimensions and the fan used were then loaded into a thermal analysis tool for thermal resistance verification. The analytical, simulated and experimental model yielded a thermal resistance of 2.5 K/W, 2.47 K/W and 2.44 K/W respectively. This indicates that the procedure of optimization can be implemented as a proven guideline to reduce the weight with optimal heat transfer.

One paper titled “Sub-Optimum Design of Forced Air Cooled Heat Sink for Simple Manufacturing” discusses maximizing the power density of a converter with a focus on minimizing the size of the heat sink. The paper studied a few different fin geometries and compared different configurations for fins and fans. The report also compared testing results for Copper and Aluminum heat sinks. In one case, a Copper heat sink was found to be 15 % more thermally resistant than its Aluminum counterpart, but it was also 4 times the weight. The study concluded that Aluminum proved to be better than Copper in the overall improvement of power density for the 5 different heat sink configurations that were looked at. In this study, Kolar and Drofenik also remarked that the largest constraint in designing heat sinks is the limited manufacturing size of

Aluminum and Copper Sheets. The paper suggested that if the fins could be thinner, the power density would improve significantly [6].

## 2.3 Customer's Need Statement

Currently, the customer has developed a heat sink for an electrical converter capable of cooling eight power modules operating at a max temperature of 150°C. The current heat sink system uses a fin type design with several cooling fans oriented horizontally along each side. This design once installed into an electrical converter contributes up to 50% of the total weight and takes up a large amount of space. These characteristics reduce the amount of electrical components that can be installed in the converter, which also reduces its efficiency. It is also currently over-designed as the bottom of the fins on the heat sink remain cool throughout all operation.

“The current heat sink system is over designed and takes up too much space and is too heavy once installed under the electrical converter.”

## 2.4 Project Objectives and Goals

This project will aim towards creating a cost effective lightweight thermal structure for future photovoltaic converters. This will allow for easier and faster installation time of the future PV converters. Figure 1, shown below, shows a high level diagram of the responsibilities for both electrical engineering students and the mechanical engineering students. Each subset of students has been performing their respective research in order to complete their portion of the overall project. After the students of the electrical or mechanical engineering discipline complete their individual tasks and responsibilities, the two teams will combine their work for testing of the final result. Collaboration between the two disciplines has been crucial in the early stages of planning to ensure that the team is headed in a cohesive direction.

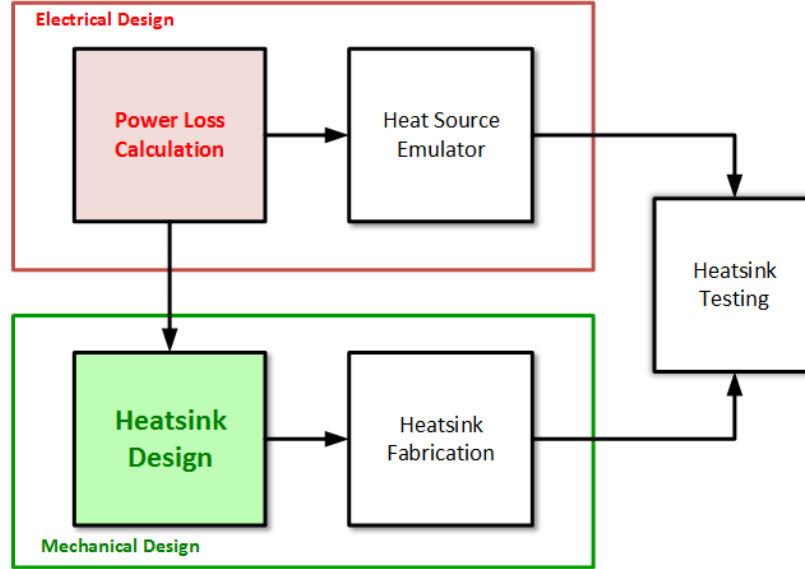


Figure 1 – Responsibilities of EE and ME Students (Image Courtesy of Thierry Kayiranga)

## 2.5 Project Constraints

These constraints are set by the sponsor and are targeted towards the customer's needs.

- Heatsink must be made of aluminum alloy
- Heatsink must weigh less than 6.5 kg
- Prevent up to eight power modules from exceeding 120°C
- Reduce size of current design
- Heatsink must have a maximum thermal resistance below 0.475 K/W

## 3. Scheduling

In order to keep its members on task and to manage different elements of the project effectively, Team 13 developed work breakdown structure for the project. The major components of the project were laid out in Figure 1. To reiterate, they include power loss calculations, heat source emulators, heatsink design and fabrication, and finally heatsink testing, or optimization. The elaborate work breakdown structure which assigns subtasks to the main components for this project is provided in Figure 2 below. Components that have been completed are highlighted in

yellow. Components that are in progress are highlighted in blue and components that have not begun are not highlighted.

Table 1 – Work Breakdown Structure

Designing & Testing a Lightweight Heatsink for a PV Converter	Power Loss Calculations	Review Documents
		Obtain Specifications
		Determine Procedure for Solving
		Perform Calculations
	Heat Source Emulation	Research Comparable Heat Sources
		Decide Materials
		Design Emulator
		Procure Materials
	Heatsink Design	Review Documents
		Collect Current Heatsink Parameters
		Comparative Heatsink Testing
		Decide Fin Type
		Perform Simulation Analysis
		Find Best Fan Configurations
		Determine Fan Attachment Methods
	Heatsink Fabrication	Finalize CAD Design
		Decide Heatsink Materials
		Procure Material
		Machine Parts
	Optimization	Test Heatsink
Compare Results to Simulations		
Iterate Design Process		

Following assigning subtasks to the major components, Team 13 organized a Gantt chart which established approximately how much time must be dedicated to each element, as well as when those tasks should begin and end. The Gantt chart (shown in Figure 2) also established precedence to necessary tasks, which is indicated by arrows. The colors on the chart indicate the different groups of team members that will be mainly responsible for each task. It should be noted that these deadlines are tentative, as unexpected circumstances can arise. Currently, the mechanical engineering students and the electrical engineering students in Team 13 are working on discipline specific tasks, but soon the team will be collaborating more as a whole. At this stage, the heatsinks testing is about to begin, and simulations have been set up in COMSOL. Calculations for determining the thermal resistances and weight have been set up in Mathcad and Matlab for the pin and plate fin heatsinks. The testing phase has begun so experimentally determined thermal resistance will be finished shortly, as well.

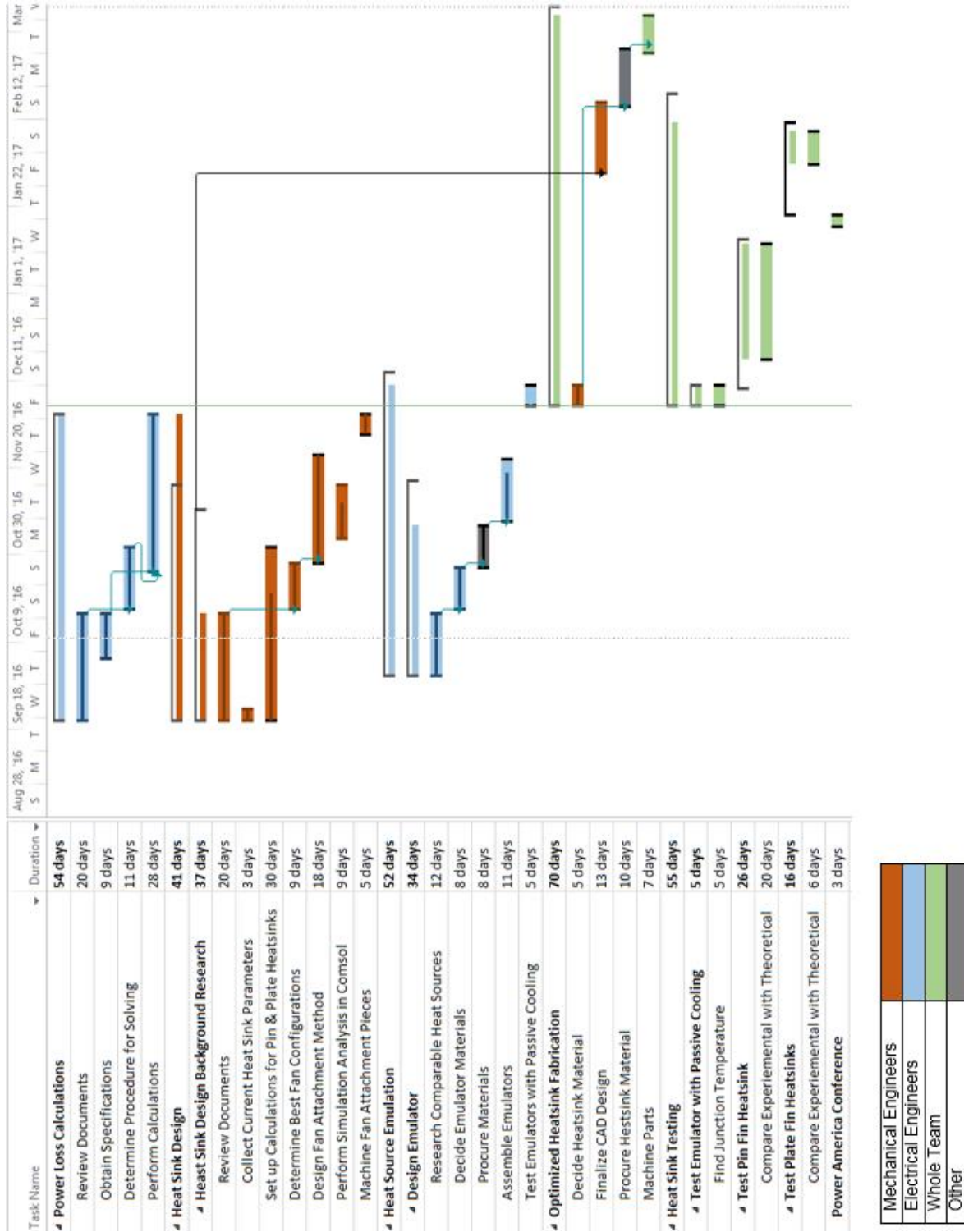


Figure 2 – Gantt Chart

## 4. Resource Allocation

Team 13 is led by Melanie Gonzalez. She is responsible for managing the team as a whole. This includes delegating tasks among the rest of the team members, finalizing all documents, planning and organizing team meetings with and without the sponsor, and overall project plans and progress. As well as being team leader, Melanie is also the lead electrical engineer and is responsible for the electrical design in support of the project. During the course of the project, Melanie will be responsible for the design of the heat source emulator that will be used to test the heatsink designed by the mechanical team.

Colleen Kidder, lead mechanical engineer, is responsible for the mechanical design in support of the project. She will be responsible for the simulation of the heatsink designs and the heat transfers analysis of the different heatsink designs using COMSOL. She will also oversee all testing done with the heatsink in the lab.

The financial advisor, Tianna Lentino, is responsible for managing the budget, maintaining a record of all credits and debits to the project account, and reviewing and analysis of expenditure requests. Tianna will also be responsible for calculating the power loss of the power modules.

Leslie Dunn is the webmaster and visual expert. She is responsible for developing and maintaining a website that follows the team's progress throughout the project. She will also be responsible for compiling any presentations and visual charts. Leslie will complete the calculations needed for the heatsink, along with determining the thermal resistances of the heatsinks.

Project 13 is a design project that will utilize computer aided design (CAD) software to create the heatsink designs. James Hutchinson is the lead CAD designer of this project. He is responsible for overseeing and finalizing all CAD designs related to the project. During the course of the project, James will also be responsible for calculating the pressure drop of the heatsink.

## 5. Product Specification

### 5.1 Design Specification

The heatsink weight is a crucial aspect of its design for this project. The weight of the current heatsink created by CAPS researchers, shown in Figure 3, is 6.45 kg. To increase the power density, the weight of the heatsink must be lowered. Therefore, optimizing the weight is largely the focus of the heatsink design process. The current heatsink, which is a plate-fin design, has a size of 279.4mm by 374.65mm, 24 fins evenly spaced, and 8 fans. The fans are arranged with 4 on each side of the heat sink. The heatsink has much more material than is necessary to keep the power modules cool and, therefore, is overdesigned.

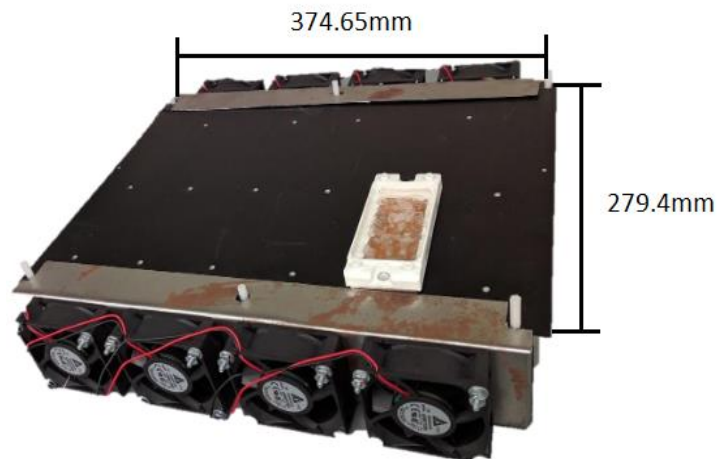


Figure 3 – Heat Sink designed by CAPS researchers

### 5.2 Performance Specification

The current heatsink is over-designed, which can be observed when the power modules are in operation and the bottom of the heat sink is cool to the touch. The heatsink system that CAPS has developed has a power density of 2.5 kW/kg. Team 13 aims to design an improved heatsink that will have a power density of 5 kW/kg. The current design has two stages of power modules. Stage 1 consists of 2 modules laid horizontally along the top of the baseplate and these modules



have an efficiency of 98.5%. Stage 2 has 6 modules laid vertically under stage 1 and have an efficiency of 97.0%. The modules each have a power loss of approximately 60W. The maximum allowable junction temperature for the power modules is 150°C.

## 6. Conceptual Design

### 6.1 Emulated Heat Source

The power modules have a 60W power loss that physically manifests as heat generated. To emulate this loss, a heat source will be constructed with resistors resting on a copper plate. The temperature threshold of the resistor will be taken into account to ensure they will operate at the desired 120°C. Resistors will be mounted to the copper plate via thermal grease to ensure maximum thermal conductivity is achieved. To mimic the power module as closely as possible, the emulated heat source will be attached to the heatsink in the same manner – resting directly on the heatsink and secured with screws. The heat dissipation of these resistors will be measured with a K-type thermocouple placed between the heatsink baseplate and the copper plate. A thermal imaging camera will be used to view the overall heat dissipation of the emulated heat source.

#### 6.1.1 Testing of Emulated Heat Source

The emulated heat source will be tested on a prototype heatsink at a single operating point of 60W loss. The appropriate voltage of about 24 V will be applied to the terminals of the heat source which will translate to about 2.5A of current flowing through the resistors. The purpose of testing the emulated heat source is to determine the heatsink thermal resistance based on equation (1). This will be determined by measuring the junction temperature,  $T_j$ .  $T_a$  is the ambient temperature,  $P_d$  is the power dissipated,  $R_{jc}$  is the thermal grease thermal resistance,  $R_{ch}$  is the power module resistance, and  $R_{ha}$  is the desired heatsink thermal resistance.

$$\frac{T_j - T_a}{P_d} - R_{jc} - R_{ch} = R_{ha} \quad (1)$$

## 6.2 Heatsink Design

For the overall design concepts, it was concluded that a bi-modular concept would be the best choice in reducing the weight and producing the heat transfer needed to dissipate the heat from the power modules. This concept will implement a total of 4 separate heatsinks each with a total of two power modules operating on the base. Even though the original heat sink housed all of the necessary power modules, about 15% of its surface area was unused and only increased the weight of the system. By implementing a bi-modular design, the unused area can be eliminated and thus decreasing the overall weight.

Another important aspect of the bi-modular design would also be its potential for an increase in overall heat transfer. Due to its smaller size, the channels for airflow will also be reduced. This ensures that a constant flow of cool air supplied by the fans which will quickly enter and exit through the heatsink. The longer channels in the previous heatsink had the potential to increase the air temperature as the air would have taken a longer time to travel throughout the entry and exit points. This increase in air temperature would have had negative effects on the air flow characteristics and the heat transfer. By choosing a bi-modular concept, Team 13 can ensure that unnecessary weight and undesired air flow can be kept to a minimum. All design concepts will be made from Aluminum T-5 6063 due to its high thermal conductivity, low density, light weight, high thermal conductivity, low cost, and manufacturability. Both plate fin and pin fin heatsink designs have been analyzed for comparison. The plate fin heatsink selected for study has 9 rectangular fins and a length, width, and height of 127mm x 127mm x 69.2mm. The pin fin heatsink has 313 small circular fins and an overall length, width, and height of 113.7mm x 113.7mm x 17.8mm. The pin fin also has a staggered design in which the spacing between the rows of fins alternate, rather than being equidistant. Important geometric parameters of each heatsink are shown numerically in Table 2.

Table 2 – Plate Fin &amp; Pin Fin Geometric Parameters

<b>Geometric Parameters</b>	<b>Plate Fin</b>	<b>Pin Fin</b>
Length	127 mm	113.7 mm
Depth	127 mm	113.7 mm
Height	69.2 mm	17.8 mm
Base Thickness	6.4 mm	4.7 mm
Fin Height	62.8 mm	13.1 mm
Fin Thickness/ Diameter	2.5 mm	3.2 mm
Fin Spacing	13.2 mm	Inline: 9 mm
		Staggered: 4.5mm
# Fins	9	313
Weight with Fans	954 g	553 g

## 6.2.1 Bi-modular Pin Fin

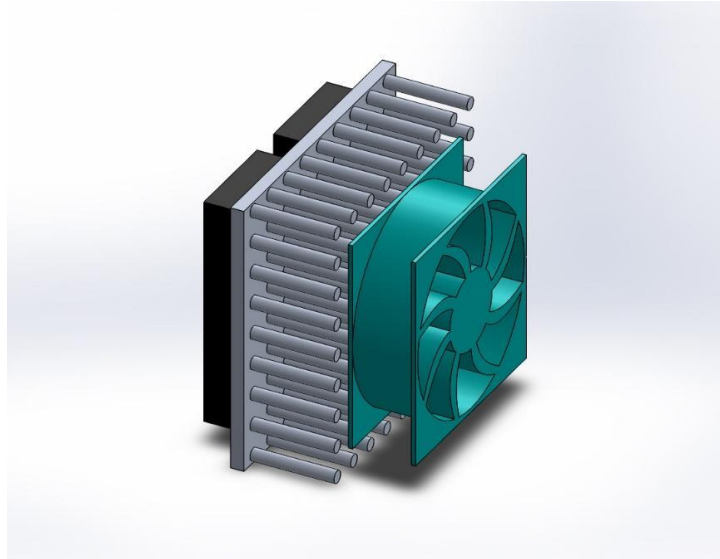


Figure 4 – Bi-modular Pin Fin Design

The bi-modular pin fin design is composed of a base that is 5mm thick with dimensions 128mm x 131mm. On the underside of the base, circular pins of constant cross section and constant spacing are evenly distributed along the entire bottom area of the base. The fan, which is used for forced convection cooling, is placed axially along the bottom of the pins. Two power modules will be placed along the topside of heatsink. Due to the pins circular design, air flow introduced into the heat sink will enter the turbulent regime, increase the mixing of the air which will remove heat at a quicker rate.

However, due to the fan being mounted axially along the base, a larger dimensioned fan will be needed to cover a larger amount of area for airflow. This has the potential for increasing the weight of the fan making it an important issue when trying to remain inside the weight constraint. The fan is to be mounted in a manner where any fasteners, screws or bolts do not impinge on the pins and without changing the overall geometry of the heat sink as well. Team 13 has developed a bracket to connect the fan to the heatsink, which is shown in Figure 6. One

challenge that team 13 faces with this heatsink is in the analytical calculations. Since the airflow going through the heat sink is in the turbulent regime, highly complicated equations are needed to determine the pressure drop and overall thermal resistance of the system. Due to the unpredictability of the turbulent regime, calculated values could differ significantly from actual experimental values. This could lead to an undesirable model for fabrication. Team 13 is still brainstorming ways to reduce the error in these calculations.

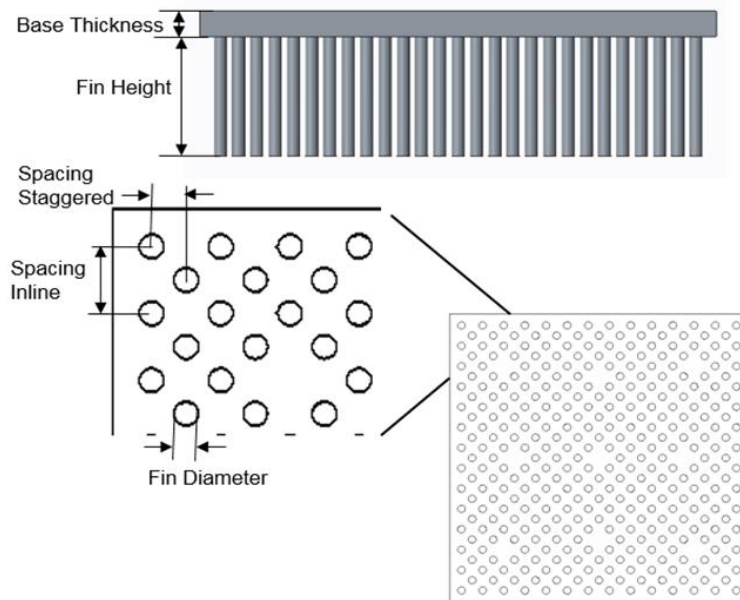


Figure 5 – Important geometric features of staggered pin fin heatsink

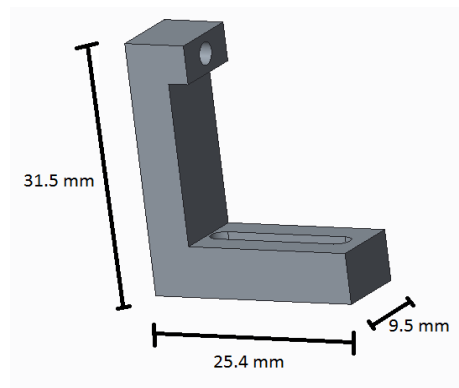


Figure 6 – Brace for Pin Fin Design

The pin fin heatsink was analyzed with a fan positioned in first the lateral direction and then the axial direction. Ideally, the fan should be mounted axially in which air flows down over the top of the pins for the best thermal performance. The 12Vdc fan for the pin fin has a size of 120mm x 120mm x 38mm, a weight of about 300 g, and a volumetric flow rate of 3.03 m<sup>3</sup>/min. A connector bracket was designed as a way to axially fix the fan to the heatsink. Four connectors were machined out of aluminum. One side of the connector was attached to the heatsink by a screw threaded into the side of the baseplate; the fan was fastened to the other side of the connector to constrain it to just below the pins.

## 6.2.2 Bi-modular Plate Fin

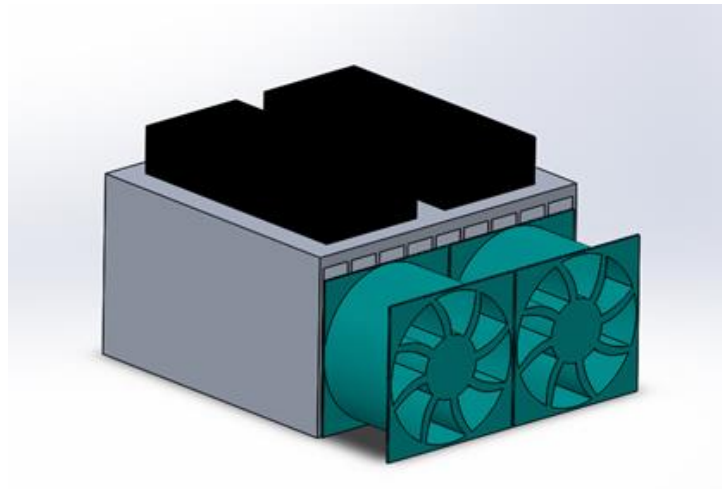


Figure 7 – Bi-modular Plate Fin Design

The bi-modular plate fins design, though similar to design 1, contains different geometry in the type extruded fins used. This design is composed of the same 5mm thick 128mm x 131mm base however thin rectangular fins are extruded through underside of the base. Each of these fins has a constant thickness and spacing along the along the base of the heat sink. Two cooling fans will be placed laterally along the side of the heat sink to allow for forced convection through the fin channels. Two power modules, just like the first design, will be placed on top on the heat sink entailing 4 will need to be fabricated.

This design contains two main advantages, one being that the air flow will act in the laminar regime making the analytical process less complicated and more in line with experimental testing. However, there will be a slight decrease in heat transfer due to the laminar airflow. The manufacturability of the design is also an advantage as plate fin heat sinks are cheaper and more customizable as compared to their pin fin counterparts. This advantage will help Team 13 significantly as the more customizations will result in more possible configurations for reducing the weight of the heat sink, and the low cost will help maintain Team 13 within the budget. However, one disadvantage of this design will be the possible decrease in heat transfer.

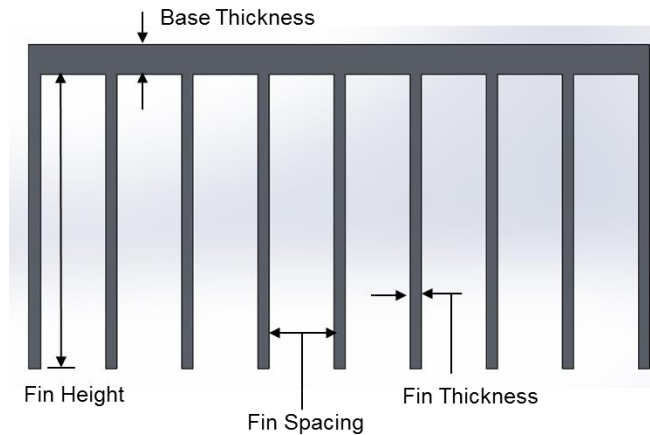


Figure 8 – Important geometric features of plate fin heatsink

For the plate fin, a 12Vdc fan was selected in order to generate forced convection through the heat sink in the lateral direction. The fan has a size of 70mm x 70mm x 25mm, a weight of 90 g, and a volumetric flow rate of 1.73 m<sup>3</sup>/min. Two of these fans were used for the plate fin heatsink.

### 6.2.3 Analysis of Plate Fin and Pin Fin Designs

Analysis was conducted for both Bi-Modular designs assuming steady-state heat transfer, incompressible air flow, and an ambient temperature of 20°C. The analysis included mathematical formulas to obtain the thermal resistance and pressure drop along with COMSOL simulations to

determine the base junction temperature. The overall weight of the designs were determined through SolidWorks program and product specification sheets.

The plate fin heatsink was determined to have a weight of 0.954 kg, a pressure drop of 7.406 Pa, a thermal resistance of 0.335 K/W, and a junction temperature of approximately 41°C. The pin fin heatsink was analyzed assuming the fan was aligned laterally and had the same flow rate as the fan used for the plate fin. The pin fin heatsink was determined to have a weight of 0.253 kg, a pressure drop of 127.4 Pa, a thermal resistance of 0.3973 K/W, and a junction temperature of about 33°C. The calculations for these values are included in a Matlab code in Appendix B. With these values known, a baseline is able to be made for the experimental testing of the two designs.

## 6.3 Heatsink Optimization

In order to design the optimal heatsink for two power modules, the most important parameters to minimize are the weight of the heatsink and the thermal resistance. This can be a complicated task because certain parameters that can enhance heat transfer (such as increasing the length of the fins) will increase the weight of the system. An overview of parameters that influence heat transfer and weight are shown in figure 9. These parameters are characteristics of the extruded fins only, and do not consider variations in the base plate of the heatsink.



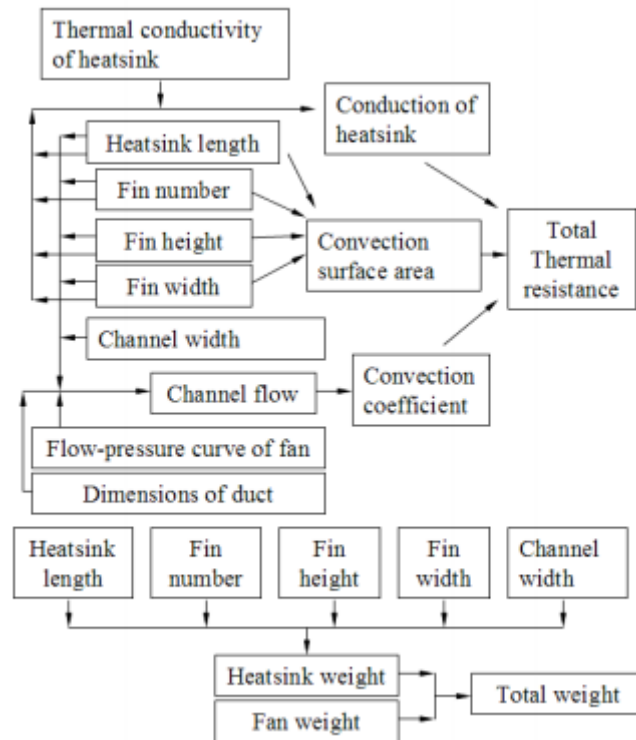


Figure 9 – Parameters that affect Thermal Resistance & Weight [5]

In order to minimize the complexity of optimization, Team 13 has decided to set certain parameters as constants while varying others. The parameters that will be held constant in mathematical simulations include the length and width of the baseplate, and the speed of the fan. It is assumed that the air flow from the fan covers the entire area that's being analyzed. The fan speed selected for calculations was  $1.74 \text{ m}^3/\text{min}$  which is based on a fan that team 13 has for testing. The base plate length and width were chosen to be  $113.7 \text{ mm} \times 113.7 \text{ mm}$ . This size was determined taking into consideration the minimum distance between modules ( $15 \text{ mm}$ ) and the size of the modules ( $108 \text{ mm} \times 46 \text{ mm}$ ). With two modules placed next to one another, the total area is  $108 \text{ mm} \times 107 \text{ mm}$  which will fit on the baseplate with  $5\text{-}6 \text{ mm}$  to spare. It is important to minimize the size of the baseplate because that is where the majority of the weight is concentrated. It should also be noted that this is the same size as a heatsink that has been ordered for testing.

For the calculations, the parameters to be varied include the baseplate thickness, the number of fins, the thickness or diameter of those fins, and their length. It should be noted that the thickness or diameter of the fins effects the channel width, and therefore the air flow through those channels and pressure drop between those channels.

For the first comparative analysis on a plate and pin fin heatsinks, it was decided that the team would test two different base thicknesses, two different numbers of fins, 3 different fin thicknesses or diameters, and 3 different fin lengths. With all these varying parameters, a total of 36 different heatsink configurations could be made for each respective heatsink type. Sample calculations for the plate fin heatsink are included in Appendix A and sample calculations for the pin fin heatsink are included in Appendix B.

## 7. Procurement

At the end of the Fall 2016 semester, Team 13 is still within budget. The materials purchased include 50 W, 5-ohm power resistors that will be used to generate the heat for the heat source emulator, screws and nuts that will hold all the components of the heat source emulator in place and will secure the heat source emulator to the heatsink, and lastly a pin fin heatsink was purchased to compare to the plate fin heatsink that the team acquired from the start of the project. Table 3 provides a list of the materials purchased during the fall semester, where the materials were ordered from, the quantity and price of the materials, and the amount of money left in the budget. Continuing into the Spring 2017 semester Team 13 will have \$277.31 remaining in the budget.

Table 3 – Budget Information for Team 13

<b>Total Budget:</b>	<b>Order Cost:</b>	<b>Ordered From:</b>	<b>Item Description:</b>	<b>Quantity:</b>
\$400.00	\$37.29	Mouser Electronics	50W 5Ω Power Resistors	10
	\$77.00	Cool Innovations	Pin Fin Heatsink	1
	\$8.40	McMaster-Carr	Steel Screws 4-40 Thread, 3/4" Length	100
		McMaster-Carr	Steel Hex Nut, 4-40 Thread Size	100
<b>Remaining Budget:</b>	\$277.31			

## 8. Risk Assessment

During the course of this project there are some risks that Team 13 had to be aware of. These risks could occur while the team is constructing or reconstructing the heat source emulator or the heatsink. In order to assemble the heat source emulator, the team will have to solder two power resistors together. Soldering components could result in burns to the person that is doing the soldering or it could result in a fire if caution is not taken. Other risks that could come from the heat source emulator include the risks that go along with securing the heat source emulator to the heatsink via power drill. If the team is not careful while drilling the holes into the heatsink, the student could slip and mistakenly hit their fingers or hand. The heatsink will be constructed with aluminum, while cutting or manipulating the material there is risk for cuts or missing fingers. While testing the heatsink and the heat source emulator there is a risk of burns do to the high

temperatures being generated by the heat source emulator. Also, since dealing with circuitry, there is a risk of a component blowing up which could cause a fire as well as electric shock when connecting the power supply to the heat source emulator. Special care will be taken when connecting the power supply by only working with one hand and wearing insulated shoes.

## 9. Conclusion

Team 13 aims to reduce the weight of a heatsink provided by CAPS researchers. By doing so, will increase the overall power density of the PV converter system with the heatsink employed from 2.5W/kg to 5W/kg. Through extensive research, the mechanical team has selected two possible heatsink designs to conduct further analysis and testing. These designs were a bi-modular pin fin design, and a bi-modular plate fin heatsink design. In order to further narrow down the concepts for the heatsink design and to allow the team to make the best possible decision, testing of both the designs will be completed and analyzed. The next steps of this project will include experimental testing, design selection, optimization and finalizing the design. Materials will be ordered based upon the results of the optimization procedure and finalized parameters, and then the final build and testing of the system will take place.

## References

- [1] Y. Xiong, S. Sun, H. Jia, P. Shea and Z. John Shen, "New Physical Insights on Power MOSFET Switching Losses," in *IEEE Transactions on Power Electronics*, vol. 24, no. 2, pp. 525-531, Feb. 2009. URL: <http://ieeexplore.ieee.org/stamp/stamp.jsp?tp=&arnumber=4783535&isnumber4783511>
- [2] X. Li, L. Zhang, S. Guo, Y. Lei, A. Q. Huang and B. Zhang, "Understanding switching losses in SiC MOSFET: Toward lossless switching," *Wide Bandgap Power Devices and Applications (WiPDA), 2015 IEEE 3rd Workshop on*, Blacksburg, VA, 2015, pp. 257-262. URL: <http://ieeexplore.ieee.org/stamp/stamp.jsp?tp=&arnumber=7369295&isnumber=7369025>
- [3] K. A. M. Annuar and F. S. Ismail, "Optimal pin fin arrangement of heat sink design and thermal analysis for central processing unit," *Intelligent and Advanced Systems (ICIAS), 2014 5th International Conference on*, Kuala Lumpur, 2014, pp. 1-5. URL: <http://ieeexplore.ieee.org/stamp/stamp.jsp?tp=&arnumber=6869537&isnumber=6869438>
- [4] U. Drogenik, A. Stupar and J. W. Kolar, "Analysis of Theoretical Limits of Forced-Air Cooling Using Advanced Composite Materials With High Thermal Conductivities," in *IEEE Transactions on Components, Packaging and Manufacturing Technology*, vol. 1, no. 4, pp. 528-535, April 2011. URL: <http://ieeexplore.ieee.org/stamp/stamp.jsp?tp=&arnumber=5725173&isnumber=5746823>
- [5] Puqi Ning, Guangyin Lei, F. Wang and K. D. T. Ngo, "Selection of heatsink and fan for high-temperature power modules under weight constraint," *Applied Power Electronics Conference and Exposition, 2008. APEC 2008. Twenty-Third Annual IEEE*, Austin, TX, 2008, pp. 192-198. URL: <http://ieeexplore.ieee.org/stamp/stamp.jsp?tp=&arnumber=4522721&isnumber=4522647>
- [6] U. Drogenik and J. W. Kolar, "Sub-Optimum Design of a Forced Air Cooled Heat Sink for Simple Manufacturing," *Power Conversion Conference - Nagoya, 2007. PCC '07*, Nagoya, 2007, pp. 1189-1194. URL: <http://ieeexplore.ieee.org/stamp/stamp.jsp?tp=&arnumber=4239306&isnumber=4239118>
- [7] W. A. Khan, J. R. Culham and M. M. Yovanovich, "Modeling of Cylindrical Pin-Fin Heat Sinks for Electronic Packaging," in *IEEE Transactions on Components and Packaging Technologies*, vol. 31, no. 3, pp. 536-545, Sept. 2008. URL: <http://ieeexplore.ieee.org/stamp/stamp.jsp?tp=&arnumber=4609948&isnumber=4627521>

## Biography

Melanie Gonzalez is a fifth-year senior engineering student studying electrical engineering. Her interests include control systems and embedded microprocessor design. She previously worked as an undergraduate research assistant at the Center for Advanced Power Systems. After graduation, she plans to work while obtaining a Master's in Electrical Engineering.

Tianna Lentino is a fourth year senior electrical engineering student. Her interests include systems engineering and power systems engineering. She has spent the past two summers working as an intern with Northrop Grumman. After she graduates, Tianna plans on working with aircraft systems.

James Hutchinson is a fifth year senior attending Florida State University, studying mechanical engineering. He is a member of the National Society of Black Engineers, Golden Key Honor Society and the Foundations Chair of the Society of Engineering Entrepreneurs. His interests include CAD design, thermal fluids, and robotics. After graduation he plans on working in either the energy or aerospace industry.

Colleen Kidder is pursuing a bachelor's degree in mechanical engineering and will graduate in May 2017. She is most interested in mechanics & materials and thermal fluids. Through internship experience at Crane Aerospace & Electronics, Colleen has developed engineering skills in a business environment. Upon graduation, she plans to take the Fundamentals of Engineering exam and begin her career at a preeminent company.

Leslie Dunn is a fifth year senior at Florida State University pursuing her B.S. in mechanical engineering. She works part-time at the FSU Central Utilities Plant where she's been conducting engineering work for a back-up fuel conversion. She has also held chair positions with the FAMU/FSU Society of Women Engineers for 3 years and is their current Vice President. Her main interests are in renewable energy, materials science, and robotics. After graduation, she wants to work with a company that focuses on sustainability.

## Appendix A: Plate Fin Calculations

For a rectangular plate fin heat sink with the fan mounted so that the air flows parallel to the fins, a procedure has been developed for determining the thermal resistance of that heatsink. Because heat transfer is highly influenced by air flow, the pressure drop over the fins must first be determined. In order to do so, a variety of parameters must be calculated. These include the Reynolds number, the coefficients of sudden expansion and contraction, the aspect ratio, and the apparent friction factor, and the hydraulic diameter. From there, the pressure drop can be calculated and then plotted vs. the volumetric flow rate of air. The line from this plot is then compared to the air flow versus static pressure curve for a specific fan. At the point where those lines would intersect, the pressure drop is found.

Once the pressure drop is determined, the heat transfer coefficient can be calculated. It is a function of the Reynolds Number, Modified Reynolds Number, Nusselt Number and Prandtl Number. With the heat transfer coefficient known, the thermal resistance of the heatsink can be found. Sample calculations for finding the pressure drop and the thermal resistance are given as follows. It should be noted that these mathcad files have been used several times with varied geometries and may not produce the exact results described in the report because of this. The procedure to find those results described has remained consistent though.

## PLATE FIN PRESSURE DROP

### Culham & Muzychka

A commercially bought fan with a stated flow rate will not actually be obtained due to the air pressure needed to force the air through the fin channels. The intersection between the commercially available fan curve and the analytical flow resistance curve indicates the operating point of the system. This point represents the actual air volume that will actually pass through the heat sink fin channels.

Len = Length of heatsink channels in flow direction

Wid = Width of Heatsink

Ht = Total Height

Baseplate thickness = 5.0mm

Height of fins = 60.0mm

tf = Thickness of fins

b = Spacing of fins/channel width

Nfin = Number of fins

Hydraulic diameter( $D_h$ ) =  $2 \times$  channel width

$K_e$  = Coefficient of Sudden Expansion

$K_c$  = Coefficient of Sudden Contraction

$\sigma$  = ratio of flow channels to that approaching heatsink

$\dot{V}$  = Volumetric flow rate of fan

$f_{app}$  = Apparent friction factor

$Re_n$  = Reynolds number

$L_{prime}$  = (Length of Heatsink/ Hydraulic Diameter)/Reynold's number

$\lambda$  = Aspect ratio (channel width/height of fin)

$\rho$  = Air density in kg/m<sup>3</sup>

$V_{av}$  = Air velocity in m/s

$\mu$  = dynamic viscosity in Pa\*s

$\Delta P$  = Pressure drop in pascals



$$\rho := 1.255 \frac{\text{kg}}{\text{m}^3} \quad \mu := 1.983 \cdot 10^{-5} \text{ Pa}\cdot\text{s}$$

Variable

$$\text{Base}_t := 4.7\text{mm}$$

$$\text{Nfin} := 15$$

$$\text{tf} := 1\text{mm}$$

$$\text{Hf} := 15\text{mm}$$

$$b := \frac{\text{Wid} - (\text{Nfin} \cdot \text{tf})}{\text{Nfin} - 1} = 7.05\text{mm}$$

$$\text{Dh} := 2 \cdot b = 0.014\text{m}$$

$$\text{Vav} := \frac{\text{Vdot}}{\text{Nfin} \cdot b \cdot \text{Hf}} = 20.529 \frac{\text{m}}{\text{s}}$$

$$\text{Ren} := \frac{\rho \cdot \text{Vav} \cdot \text{Dh}}{\mu} = 1.832 \times 10^4$$

$$\text{Lp} := \frac{\left(\frac{\text{Len}}{\text{Dh}}\right)}{\text{Ren}} = 4.402 \times 10^{-4}$$

$$f := \frac{\left(24 - 32.527 \cdot \lambda + 46.721 \cdot \lambda^2 - 40.829 \cdot \lambda^3 + 22.954 \cdot \lambda^4 - 6.089 \lambda^5\right)}{\text{Ren}} = 8.611 \times 10^{-4}$$

$$f_{\text{app}} := \frac{\left[\left(\frac{3.44}{\sqrt{\text{Lp}}}\right)^2 + (f \cdot \text{Ren})^2\right]^{0.5}}{\text{Ren}} = 8.992 \times 10^{-3}$$

$$\Delta P := \left(K_c + 4 \cdot f_{\text{app}} \cdot \frac{\text{Len}}{\text{Dh}} + K_e\right) \cdot \frac{\rho \cdot \text{Vav}^2}{2} = 120.135 \text{ Pa}$$

$$\text{mmh20} := \Delta P \cdot \frac{0.101971621298 \cdot \text{mm}}{\text{Pa}} = 0.482\text{-in}$$

Fixed

$$\text{Vdot} := 69 \frac{\text{ft}^3}{\text{min}} = 0.033 \frac{\text{m}^3}{\text{s}}$$

$$\text{Len} := 113.7\text{mm} \quad \text{Wid} := 113.7\text{mm}$$

$$\text{Ht} := \text{Base}_t + \text{Hf}$$

$$\sigma := 1 - \frac{\text{Nfin} \cdot \text{tf}}{\text{Wid}} = 0.868$$

$$K_c := 0.42 \cdot (1 - \sigma^2) = 0.104$$

$$K_e := (1 - \sigma^2)^2 = 0.061$$

$$\lambda := \frac{b}{\text{Hf}} = 0.47$$

## Total Thermal Resistance of Plate Fin Heatsink

Hf = Height of Fin  
Hb = Height of Base  
Wid = Width of Fin  
Len = Length of Fin Channels  
Nfin = Number of Fins  
Vdot = Volumetric Flow Rate of Fan  
 $\mu$  = Kinematic Viscosity  
b = channel width  
tf = Thickness of Fin  
kf = Thermal conductivity of air  
k = Thermal conductivity of Heat sink material  
Pr = Prandtl Number

Vav = Channel Velocity  
Res = Reynolds Number  
modRen = Modified Reynolds Number  
Nu = Nusselt Number  
h = Convection Coefficient  
Ra = Convection Thermal Resistance  
Rfin = Conductive thermal resistance of fin  
Rd = Conductive Thermal Resistance of Base  
Rtotal = Total Thermal Resistance

$$\text{Len} := 118\text{mm}$$

$$\rho := 1.255 \frac{\text{kg}}{\text{m}^3}$$

$$\text{Pr} := 0.713$$

$$\text{Wid} := 125\text{mm}$$

$$\text{Hb} := 5\text{mm}$$

$$\nu := 15.11 \cdot 10^{-6} \frac{\text{m}^2}{\text{s}}$$

$$\text{Vdot} := 68.0 \frac{\text{ft}^3}{\text{min}}$$

$$\text{Hf} := 60\text{mm}$$

$$\text{Ht} := 69.85\text{mm} + 6.35\text{mm}$$

$$k_f := 0.0257 \frac{\text{W}}{\text{m}\cdot\text{K}}$$

$$\mu := 1.983 \cdot 10^{-5} \text{Pa}\cdot\text{s}$$

$$\text{tf} := 2.42\text{mm}$$

$$k := 209 \frac{\text{W}}{\text{m}\cdot\text{K}}$$

$$\text{Nfin} := 9$$

$$b := 13\text{mm}$$

$$\text{Vav} := \frac{\text{Vdot}}{\text{Nfin} \cdot b \cdot \text{Hf}} = 4.572 \frac{\text{m}}{\text{s}}$$

$$\text{Ren} := b \cdot \frac{\text{Vav}}{\nu} = 3.933 \times 10^3$$

$$\text{modRen} := \frac{\text{Ren} \cdot b}{\text{Len}} = 433.317$$

$$\text{Nu} := \left[ \left( \frac{\text{modRen} \cdot \text{Pr}}{2} \right)^{-3} + \left( 0.664 \sqrt{\text{modRen}} \cdot \text{Pr}^{\frac{1}{3}} \cdot \sqrt{1 + \frac{3.65}{\sqrt{\text{modRen}}}} \right)^{-3} \right]^{\frac{-1}{3}}$$

$$h := \text{Nu} \cdot \frac{k_f}{b} = 26.459 \frac{\text{kg}}{\text{K}\cdot\text{s}^3}$$

$$\text{Ra} := \frac{1}{h \cdot \text{Len} \cdot \text{Hf}} = 5.338 \frac{\text{K}\cdot\text{s}^3}{\text{m}^2 \cdot \text{kg}}$$

$$\text{Rfin} := \frac{\text{Hf}}{\text{tf} \cdot \text{Len} \cdot k} = 1.005 \frac{\text{K}\cdot\text{s}^3}{\text{m}^2 \cdot \text{kg}}$$

$$\text{Rd} := \frac{\text{Hb}}{\text{Wid} \cdot \text{Len} \cdot k} = 1.622 \times 10^{-3} \frac{\text{K}\cdot\text{s}^3}{\text{m}^2 \cdot \text{kg}}$$

$$\text{Rtotal} := \text{Rd} + \frac{(\text{Rfin} + \text{Ra})}{2\text{Nfin}} = 0.354 \frac{\text{K}\cdot\text{s}^3}{\text{m}^2 \cdot \text{kg}}$$

## Appendix B: Pin Fin Calculations

### Calculations with Fan Mounted on the Side

For finding the thermal resistance of the pin fin heatsink, two different approaches were taken. The complexity of the pressure drop in between the pin fins made these calculations difficult to perform so one approach was to mimic the procedure performed by Waqar Ahmed Khan, J. Richard Culham, and M. Michael Yovanovich in “Modeling of Cylindrical Pin-Fin Heat Sinks for Electronic Packaging” [7]. This procedure, however, considered the fan mounted on the side of the pins, not axially so this team developed a method to find an upper-bound heat transfer coefficient with the fan mounted axially on the heatsink. The matlab code for the calculations is given as follows. It should be noted that this file has been used several times with varied geometries and may not produce the exact results described in the report because of this. The procedure to find those results described has remained consistent, however.

```

%% Known variables
Tamb = 20;
Tbp = 120;
P = 2*83.3;

%% Heatsink material
kf = 2.624e-5;      % Thermal conductivity of air at 300 K
k = 0.237;         % Thermal conductivity of AL
p = 2.65e-3;       % Density of aluminium
pf = 1.161e-6;     % Density of air at 300K

Rt = (Tbp - Tamb)/P; % Theoretical Rth

%% Fan specification
Lf = 113.7;
Wf = 113.7;
A = Wf*Lf;
Af = 1.74;         % Air flow
Vapp = Af*1e9/(60*A)
Wfan = 0;

%% Heat sink size
Hfin = 17.8-4.7;
tbp = 4.7;
%D = 0.5:0.1:10;
D = 3.2;
so = 2;           % Minimum distance
s = 4;

St = 2.*(D./2) + s + so

N = 113.7./St      % N = Nt = Nl
Nl = N;
Nt = N;

S1 = St;
Sd = sqrt(S1.^2 + 0.25.*St.^2);

```

```

% Fixed based on module sizes
W = 113.7;           % Width of the heatsink
L = 113.7;           % Length of the heatsink
H = Hfin + tbp;     % Height of the heatsink
y = Hfin./D;        % Slendering Ratio
Abp = (L.*W - (N.^2.*(0.25.*pi.*D.^2)));
Afin = pi.*D.*Hfin;

%% Reynolds and Prandlt Numbers
V = Vapp;
Vk = 15.68;
Pr = 0.707;
Re = V.*D./Vk;

%%
C1 = (0.2 + exp(-0.55.*(St./D))).*(St./D).^0.785.*(Sl./D).^0.212/(((St./D) - 1).^0.5);
hbp = 0.75.*(kf./L).*Re.^0.5.*Pr.^(1/3)
hfin = (kf./D).*C1.*Re.^0.5.*Pr.^(1/3)
m = sqrt((4.*hfin)./(k.*D));
nfin = tanh(m.*H)./(m.*H);

K1 = 1.009.*(((St./D) - 1)./((Sl./D) - 1)).^(1.09./(Re.^0.0553));
f = K1.*(0.233 + 45.78./(((St./D) - 1).^1.1.*Re));
Vmax = Vapp

%%
B = pf.*Vk.^3.*kf.*Tamb./P.^2;
C3 = pi.*C1.*y.*nfin + (0.75./sqrt(Nl.*(Sl./D))).*((St./D).*(Sl./D) - (pi./4));
C2 = (Tamb./N.^2.*tbp).*((Tbp./((Sl./D).*(St./D).*D)) + (1./C3.*(kf./k).*Re.^0.5.*Pr.^(1/3)));
C4 = Nt.*(St./D).^3.*f.*Nl./(((St./D) - 1).^2);

%% Entropy
Ns = (C2./Re) + 0.5.*(C4.*B.*y.*Re.^2);

%% Resistances calculations
Rc = 0; %1/(hc*Ac);
Rfin = 1./(hfin.*Afin.*nfin);
Rbp = 1./(hbp.*Abp);
Rm = tbp./k.*A;
Rfins = 1./((N.^2./(Rc + Rfin)) + (1./Rbp));

%% Thermal Resistance
Rhs = Rm + Rfins

%%
W = (p.*(tbp.*L.*W + N.^2.*pi.*D.^2.*Hfin) + Wfan)
W2 = (p.*((tbp.*L.*W) + (313.*pi*1.6^2*Hfin)))

%% Pressure Drop
dP = 0.5.*f.*pf.*Vmax.^2.*N.^2

```

## Calculations with Fan Mounted Axially

For determining the thermal resistance with the fan mounted axially, the team performed calculations for the Nusselt number considering flow over 1 cylinder. The equations for finding the nusselt number varied based on the value of the Reynolds number. The fin efficiency was calculated as well considering cylindrical fins and multiplied by the convective heat transfer coefficient. From there, the theoretical thermal resistance of the heatsink could be found. The Matlab code for these sample calculations is given.

```

clc
clear all

##### PIN FIN Heatsink
%%assume constant fin cross section & constant thermal conductivity

T_fluid = 25;    %deg Celcius           Fluid Temp
T_base = 120;   %deg Celcuiss          Desired chip temp
P = 2*83.3;     %atm                    Pressure

Q = 200;        %Watts                  Power Loss module

k_al = 237;     %W/mK                    Aluminum conductivity
density_Al= 2.65e3; % kg/m^3            density of Aluminum

##### VARIABLE #####
l_x_base = .1137; %meters                heatsink size
l_y_base = .1137; %meters                heatsink width
t_base = 0.0047; %meters                 Thickness of base
D_fin = 0.0032; %meters                  Fin diameter
r_fin = D_fin/2;

num = 304;                                %Number of Pins
%L = linspace(0, .1, 100); %meters       length of fins
L = .0178-.0047;

L_c = L + (D_fin/4);                       %corrected length

##### AREAs #####
A_pin = pi*D_fin*L_c;                       %Area of 1 fin
A_pin_top = pi* r_fin^2;                    %Area of Fin Top
A_base = l_x_base * l_y_base;               %Base Area
A_unfin = A_base - (num*A_pin_top)          %Exposed unfinned base area
A_fin_surface = (pi.*D_fin.*L)+(pi*r_fin^2) %Surface area of 1 fin
Vol = (A_base*t_base) + (A_pin_top.*L*num) %Heatsink total Volume

##### convective heat transfer coefficient approximation #####

Pr = .7296;                                %Pr air at 25 deg C
v_k = 15.62 * 10^(-6); %m^2/s             kinematic viscosity of air at 25 deg C
k_fluid = 0.02551; %W/mK                  Air conductivity at 25 deg C

```



```

V_dot = 0.032;      % m^3/s                Fan Air Flow (cfm)
V_av = (V_dot)/(A_base - (num*A_pin_top));

Re = D_fin * V_av / v_k;      %unitless    Reynolds Number

if Re >=4 && Re <= 40
    Nu = 0.911*(Re^(.385))*(Pr^(1/3));
elseif Re > 40 && Re <= 4000
    Nu = 0.683*(Re^(.466))*(Pr^(1/3));
elseif Re >4000 && Re <= 40000
    Nu = 0.193*(Re^(.618))*(Pr^(1/3));
else
    Nu=0;
end

h = Nu*k_fluid/D_fin          % Convection heat transfer coefficient

%%%%%%%%%%%%%%%%%%%%%%%%%%%%%%%%%%%%%%%%%%%%%%%%%%%%%%%%%%%%%%%%%%%%%%%%
m = sqrt((4*h)/(k_al*D_fin)); % geometry factor

Lm_degtorad = degtorad(m.*L_c); %convert to radians for matlab tanh
n=tanh(Lm_degtorad)./(m.*L_c); %efficiency

%%%%%%%%%%%%%%%%%%%%%%%%%%%%%%%%%%%%%%%%%%%%%%%%%%%%%%%%%%%%%%%%%%%%%%%%
R_conv = 1./ ( ( num.*n.*h.*A_fin_surface)+(h.*A_unfin) )
R_cond = t_base / (k_al*A_base)
R_total = R_cond + R_conv

T_c = (Q.*R_total) + T_fluid;
Weight = Vol*density_Al;
%%%%%%%%%%%%%%%%%%%%%%%%%%%%%%%%%%%%%%%%%%%%%%%%%%%%%%%%%%%%%%%%%%%%%%%%
figure(1)
subplot(3,3,1)
plot(L, T_c), grid on
xlabel('Length of fin in meters')
ylabel('Chip Surface Temperature in Celcius')
title('Length of fin vs Chip Surface Temperature ')

subplot(3,3,2)
plot(L, Weight), grid on
xlabel('Length of fin in meters')
ylabel('Weight')
title('Length of fin vs Weight')

```